Selenium attenuates ischemia/reperfusion injury-induced damage to the blood-brain barrier in hyperglycemia through PI3K/AKT/mTOR pathway-mediated autophagy inhibition

BIAO YANG*, YAQIONG LI*, YANMEI MA*, XIAOPENG ZHANG, LAN YANG, XILIN SHEN, JIANZHONG ZHANG and LI JING

Ningxia Key Laboratory of Cerebrocranial Diseases, School of Basic Medical Science, Incubation Base of National Key Laboratory, Ningxia Medical University, Yinchuan, Ningxia Hui Autonomous Region 750004, P.R. China

Received March 2, 2021; Accepted June 25, 2021

DOI: 10.3892/ijmm.2021.5011

Abstract. Ischemic stroke is a leading cause of mortality and disability. Diabetes mellitus, characterized by hyperglycemia, is a common concomitant disease of ischemic stroke, which is associated with autophagy dysfunction and blood-brain barrier (BBB) damage following cerebral ischemia/reperfusion (I/R) injury. At present, there is no effective treatment strategy for the disease. The purpose of the present study was to explore the molecular mechanisms underlying the protective effects of selenium on the BBB following I/R injury in hyperglycemic rats. Middle cerebral artery occlusion was performed in diabetic Sprague-Dawley rats. Treatment with selenium and the autophagy inhibitor 3-methyladenine significantly reduced cerebral infarct volume, brain water content and Evans blue leakage, while increasing the expression of tight junction (TJ) proteins and decreasing that of autophagy-related proteins ($P<0.05$). In addition, selenium increased the phosphorylation levels of PI3K, AKT and mTOR ($P<0.05$). A mouse bEnd.3 brain microvascular endothelial cell line was co-cultured *in vitro* with an MA-h mouse astrocyte-hippocampal cell line to simulate the BBB. The cells were then subjected to hyperglycemia, followed by oxygen-glucose deprivation for 1 h and reoxygenation for 24 h. It was revealed that selenium increased TJ protein levels, reduced BBB permeability, decreased autophagy levels and enhanced the expression of phosphorylated (p)-AKT/AKT and p-mTOR/mTOR proteins ($P<0.05$). Treatment with wortmannin (an inhibitor of PI3K) significantly prevented the beneficial effects of selenium on the BBB, whereas insulin-like growth factor 1 (a PI3K activator) mimicked the effects of selenium. In conclusion, the present findings indicated that selenium can inhibit autophagy by regulating the PI3K/AKT/mTOR signaling pathway, significantly preventing BBB damage following cerebral I/R injury in hyperglycemic conditions.

Correspondence to: Professor Li Jing or Professor Jianzhong Zhang, Ningxia Key Laboratory of Cerebrocranial Diseases, School of Basic Medical Science, Incubation Base of National Key Laboratory, Ningxia Medical University, 1160 Shengli Street, Yinchuan, Ningxia Hui Autonomous Region 750004, P.R. China
E-mail: jingli_nxmu@163.com
E-mail: zhangjz@nxmu.edu.cn

*Contributed equally

Key words: selenium, cerebral ischemia/reperfusion, hyperglycemia, blood-brain barrier, autophagy, PI3K/AKT/mTOR

Introduction

Ischemic stroke, accounting for ~85% of all cases of strokes (1), is a leading cause of mortality and disability (2,3). Diabetes mellitus (DM), characterized by hyperglycemia, is an important risk factor for ischemic stroke, and ~30% of patients with stroke have diabetes (4). Hyperglycemia can cause microvascular lesions, and the blood-brain barrier (BBB), which acts as a semipermeable barrier between peripheral blood and the central nervous system (CNS), is damaged during the acute phase of diabetic stroke (5-7). In addition, increased vascular permeability and the spillover of macromolecules and pro-inflammatory factors can exacerbate post-stroke injury and lead to hemorrhagic transformation, posing additional therapeutic challenges (8,9). At present, tissue plasminogen activator is the only drug used for thrombolytic therapy after a stroke, but its therapeutic time window is extremely narrow, and the risk of bleeding is significant (10). Even with thrombolytic therapy, the mortality and disability rates in patients who have suffered a stroke remain high (11). Therefore, it is necessary to develop new treatments for ischemic stroke in hyperglycemic patients.

Autophagy is a physiological process characterized by the degradation and recycling of cellular components. Autophagy is activated as a survival response in hypoxic conditions, low nutrient availability and other forms of stress to remove damaged proteins and dysfunctional organelles (12). Below a certain threshold, autophagy is beneficial; however, when this threshold is exceeded, it can lead to cell death (13-15). BBB damage is a key event in the secondary

CNS damage following stroke, which is often associated with the aberrant autophagy of brain microvascular endothelial cells (16). Studies have revealed that excessive autophagy can lead to cell dysfunction and death, as shown by the activation of the autophagy pathway following oxygen-glucose deprivation (OGD), the loss of tight junction (TJ) protein expression and the increase in endothelial cell permeability (17,18). Furthermore, it has been revealed that the inhibition of autophagy significantly reduces endothelial cell permeability. Similarly, a recent study revealed that, following autophagy inhibitor intervention in a rat model of middle cerebral artery occlusion (MCAO), Evans blue (EB) leakage and TJ protein expression were increased, which protected BBB integrity (16). In a recent study, autophagy was induced in a pMCAO mouse model of ischemic stroke and oxygen-glucose deprivation intervention was performed *in vitro*, following which a significant amount of pericytes (important constituent cells of the BBB) underwent cell death and BBB integrity was destroyed. The inhibition of autophagy could also significantly promote the survival of pericytes and effectively reduce BBB damage (19). Studies have revealed that autophagic activity is significantly increased and the BBB is damaged in diabetic mice following cerebral ischemia/reperfusion (I/R) injury, and that the inhibition of autophagy can attenuate brain injury (20,21). For example, a recent study revealed that apigenin attenuates brain injury by inhibiting autophagy in cerebral vascular endothelial cells, exerting a protective effect against I/R injury (22). In addition, icariside II can inhibit autophagy, reduce MMP9 and MMP2 levels, significantly reduce EB leakage following cerebral I/R in rats and effectively alleviate BBB injury (1). The PI3K/AKT/mTOR signaling pathway has been revealed to regulate several biological processes, such as proliferation, differentiation and apoptosis (23). The PI3K/AKT/mTOR pathway has also been revealed to be closely associated with autophagy (24,25). In addition, Liu *et al* (26) demonstrated that the PI3K/AKT signaling pathway was inhibited in a hyperglycemic environment, Autophagy-related circular RNA can attenuate autophagy and ROS production in Schwann cells subjected to hyperglycemia by promoting the activation of the PI3K/AKT/mTOR pathway (27).

Selenium (symbol Se) is an essential trace element that is necessary for animal and plant health (28,29). Selenium plays an important role in antioxidation by affecting the activity of glutathione peroxidase (30,31). In addition to its antioxidative activity, selenium has become the focus of intensive research for its potential role in the regulation of autophagy. Selenium can reverse the inhibitory effect of citreoviridin on mTOR2 and inhibit autophagy in cardiomyocytes (32). Selenium can also inhibit lactate dehydrogenase (LDH) release and cadmium-induced autophagy by regulating calcium homeostasis in leghorn male hepatoma cells (33). Our previous study showed that sodium selenite exerts a neuroprotective effect by modulating autophagy-related proteins (34); however, whether it exerts a protective effect on the BBB following cerebral I/R injury in hyperglycemic conditions remains unknown.

In the present study, an *in vivo* MCAO model of diabetic rats was established by co-culturing bEnd.3 mouse brain microvascular endothelial and MA-h mouse astrocyte-hippocampal cells to simulate the BBB in hyperglycemic conditions by subjecting them to OGD/reoxygenation (OGD/R) *in vitro*. The purpose of the present study was to explore the molecular mechanisms underlying the protective effects of selenium on the BBB following I/R injury in hyperglycemic rats.

Materials and methods

In vivo experiments

Animals. All animal experiments and procedures were conducted in accordance with the Chinese Laboratory Animal Use Guidelines (35) and followed the Laboratory Animal Care and Use guidelines of Ningxia Medical University (Yinchuan, China). All animal procedures were approved by the Institutional Animal Care and Use Committee (IACUC) of the Ningxia Medical University (Yinchuan, China). A total of 100 adult male Sprague-Dawley rats (weight, 220-240 g) at 8 weeks of age were provided by Ningxia Medical University (approval no. IACUC-NYLAC-2019-064). Animals were housed under controlled temperature (22-24˚C) and humidity (60±5%) conditions in a 12-h light/dark cycle and they were allowed free access to food and water. A total of 4 weeks after the induction of diabetes with streptozotocin (STZ), the rats were randomly divided into five groups: The hyperglycemia Sham (Sham), hyperglycemia I/R (HIR), sodium selenite-treated hyperglycemia I/R (Se), 3-methyladenine (3-MA)-treated hyperglycemia I/R (3-MA) and sodium selenite plus 3-MA-treated hyperglycemia I/R (Se + 3-MA) groups (20 rats per group). For the inhibition of autophagy, 3-MA (30 μg; Merck KGaA) was dissolved in 10 μl saline (36) and injected into the ipsilateral ventricle immediately after MCAO.

Induction of diabetes. Diabetes was induced in the rats by 12-h fasting followed by intraperitoneal (i.p.) administration of STZ (60 mg/kg; Merck KGaA) (37). Blood glucose levels were assessed after 72 h, with levels of >16.8 mmol/l considered hyperglycemic. Diabetic rats in the Se group received i.p. injections of sodium selenite solution (0.4 mg/kg/day) and cerebral ischemia was induced 4 weeks later (38).

Cerebral I/R injury. Cerebral I/R injury was induced by unilateral MCAO (39). This was carried out following the induction of diabetes and sodium selenite treatment for 4 weeks. The animals were anesthetized by inhalation of 3% isoflurane (induction) and maintained with 1.5-2.0% isoflurane during surgical procedures, and the right internal carotid artery was exposed and the thread bolt was inserted. Following MCAO (30 min), the thread bolt was removed to restore normal blood flow. The sham group underwent the same procedure, but the middle cerebral artery was only exposed instead of occluding it. Immediately after the surgery, the 3-MA treatment group was intracerebroventricularly (i.c.v.) injected with 3-MA (30 μg dissolved in 10 μl saline) (36). Normal saline (10 μl) was injected in the Sham group. Successful induction was defined as the appearance of hemiplegia 24 h after MCAO. Rats were euthanized by an injection of excessive sodium pentobarbital (800 mg/kg) (40); successful euthanasia was defined as the disappearance of reflex and respiration, and cardiac arrest. Following euthanasia, the brain tissues of 6 rats from each group were randomly selected for triphenyltetrazolium

chloride (TTC) staining, and those from the other 10 rats were collected for follow-up biochemical tests.

Neurological deficit scoring. Two investigators who were blinded to the groups conducted a neurological deficit evaluation 24 h after MCAO, according to the Z-longa score grading criteria: 0, Asymptomatic; 1, left forelimb internal rotation; 2, left rotation; 3, left rotation dumping; 4, no spontaneous activity and/or exhibiting depressed levels of consciousness (41). Rats with scores of ≥2 were selected for the subsequent experiment.

Brain water content determination. The rat brains were quickly collected following anesthesia and weighed (wet weight). Next, the brains were dried at 100˚C for 24 h and weighed (dry weight) (42). The formula for calculating the brain water content was: (wet weight-dry weight)/wet weight x100%.

Infarct volume assessment. A total of 24 h after MCAO, the brains were harvested and cut into 2-mm thick coronal sections. The slices were stained with 3-5-TTC (1.5%; Merck KGaA) for 15 min at 37˚C and then fixed with 4% paraformaldehyde for 12 h at room temperature. Normal tissue appeared red, while the infarcted area was stained white. Brain sections were visualized by a digital camera and ImageJ 1.46 (National Institutes of Health) was used to assess the infarct area and correct for edema (43). The formula used for calculating the cerebral infarct volume is as follows: Cerebral infarct volume=contralateral hemispheric volume-(ipsilateral hemispheric volume-infarcted area volume).

BBB permeability evaluation. The animals were anesthetized 24 h after MCAO, and EB (2%; Merck KGaA) was injected into the tail vein at a dose of 5 ml/kg. Each hemisphere was homogenized in 50% trichloroacetic acid, followed by centrifugation at 12,000 x g for 15 min at 4˚C. Next, 1 ml supernatant was collected and the optical density value was measured at 632 nm using a fluorescence spectrophotometer (44).

Transmission electron microscopy (TEM). The penumbral cortex was collected following cerebral I/R and fixed overnight in 2% glutaraldehyde at 4˚C, followed by three washes with 0.1 M sodium dimethyl arsenate buffer. The cortex was then soaked for 2 h at 4˚C in 1% osmic acid and rinsed three times with dimethyl arsenic sodium buffer. Next, the cortex was dehydrated by immersing in a gradient series of alcohol (30, 50, 70, 80, 90 and 100%) for 10 min at each concentration at room temperature. The sample was then embedded in epoxy resin, polymerized, sliced into ultra-thin sections and placed on the copper net. Following 1% uranium acetate and 0.2% lead citrate double staining for 10 min respectively at room temperature, the sample was observed using a transmission electron microscope (magnification, x8,000; model no. H7800; Hitachi, Ltd.).

Immunofluorescence staining. Autophagy-associated proteins Beclin-1, LC3B and p62 were detected by immunofluorescence. Briefly, paraffin sections (4 μm thick) of brain tissue were incubated in 0.3% Triton X-100 for 30 min at room temperature, and then incubated overnight at 4˚C with rabbit anti-Beclin-1 (1:50; product code ab62557; Abcam), rabbit anti-LC3B (1:100; product code ab192890; Abcam) and rabbit anti-p62 (1:50; product code ab109012; Abcam) primary antibodies, followed by incubation at room temperature for 1 h with tetramethylrhodamine/FITC-conjugated anti-rabbit secondary antibodies (1:100; product code bsm-33179; BIOSS). Finally, samples were fixed with DAPI sealant (10 μg/ml; Shanghai Yeasen Biotechnology Co., Ltd.) at room temperature in the dark for 5 min and analyzed under a fluorescence microscope (magnification, x400; Olympus Corporation).

In vitro experiments

Cell identification, co-culture and treatments. The bEnd.3 mouse brain microvascular endothelial and MA-h mouse astrocyte-hippocampal cell lines were purchased from The Cell Bank of Type Culture Collection of The Chinese Academy of Sciences. Mouse anti-CD34 (1:100; product code ab54208; Abcam) and mouse anti-glial fibrillary acid protein (GFAP; 1:100; product code ab4648; Abcam) were used for bEnd.3 and MA-h cell identification, respectively; the method is similar to tissue immunofluorescence. Cells were co-cultured *in vitro* to simulate the damage to the BBB caused by hyperglycemic conditions and I/R injury (45,46). Briefly, bEnd.3 and MA-h cells were first cultured separately in DMEM/F12 (Cytiva) in an incubator (94% relative humidity, 5% CO_2 and 37˚C). Next, poly-lysine-coated Transwell (0.4 μm; Corning, Inc.) inserts were removed, and the MA-h cell line ($5x10^5$ cells/ml) was seeded into the outer chamber, cultured for 6 h, and then the chamber was turned over to be cultured for another 6 h. Next, the bEnd.3 cell line (density, $5x10^5$ cells/ml) was seeded on the insert and incubation was continued for an additional 12 h.

D-glucose (50 mM; control) and hyperglycemia + OGD/R (H + O) were used to simulate the BBB injury induced by hyperglycemic conditions and I/R injury. Prior to OGD/R, the high-sugar medium was replaced with sugar-free medium and cells were cultured in a hypoxic chamber (oxygen concentration, 1%) for 1 h (38). After 24 h of reoxygenation, cells were collected for analysis. Sodium selenite (100 nM) was added 24 h before OGD/R induction. To determine whether selenium inhibited autophagy and to determine the underlying mechanisms, 3-MA (10 nmol; Merck KGaA), wortmannin (Wort; 10 nmol; Merck KGaA; a specific PI3K inhibitor) and insulin-like growth factor 1 (IGF-1; 100 nmol ng/ml; Merck KGaA; a PI3K activator) were added to the culture medium 2 h before sodium selenite treatment. All reagents were dissolved in PBS (47) (vehicle). First, the cells were divided into the following groups: Control (hyperglycemia), H + O (hyperglycemia + OGD/R), Se (hyperglycemia + OGD/R + sodium selenite), 3-MA (hyperglycemia + OGD/R + 3-MA) and Se + 3-MA (hyperglycemia + OGD/R + sodium selenite + 3-MA) groups. Then the cells were divided into the following groups: Vehicle (hyperglycemia + OGD/R + vehicle), Se (hyperglycemia + OGD/R + sodium selenite), IGF-1 (hyperglycemia + OGD/R + IGF-1), Wort (hyperglycemia + OGD/R + wortmannin) and Se + Wort (hyperglycemia + OGD/R + sodium selenite + wortmannin) groups. All tests were repeated three times.

Cell viability assessment. Cell viability was determined using a Cell Counting Kit-8 (CCK-8) assay (Dojindo Molecular Technologies, Inc.), according to the manufacturer's

instructions. Briefly, bEnd.3 and MA-h cells were plated into a 96-well plate (5,000 cells/well) and treated with different reagents (25, 50, 100, 200 and 400 nmol sodium selenite, and 17.5, 30, 40, 50, 60 and 70 mM D-glucose). In the control group, 17.5-mM glucose diluted in DMEM/F12 medium was used. Following the addition of CCK-8 (10 μl/well, incubated at 37˚C for 2 h), the absorbance was measured at 450 nm using a microplate reader.

In vitro BBB permeability. The *in vitro* permeability of the BBB was evaluated using fluorescein sodium dye (cat. no. F6377; Merck KGaA) (48). After the co-cultured cells had fused, they were subjected to hyperglycemia (D-glucose, 50 mM) and hyperglycemia + OGD/R (H + O), and treated with sodium selenite (100 nM) and fluorescein sodium dye for 24 h. Next, 5 μg/ml fluorescein sodium was added to the upper Transwell chamber, followed by incubation at 37˚C for 30 min. Finally, 100 μl medium was collected from the basal chamber and the absorbance was measured at 485/535 nm using a spectrophotometer.

Western blot analysis. Co-cultured cells and rat ischemic penumbral tissue were collected and lysed with RIPA lysis buffer (Beyotime Institute of Biotechnology). Protein concentration was determined using the BCA protein analysis kit (Beyotime Institute of Biotechnology). Equivalent amounts of protein samples (30 μg/well) were separated by electrophoresis via 6-15% SDS-PAGE, transferred to PVDF membranes (EMD Millipore), blocked with 5% skimmed milk for 70 min at 4˚C and incubated overnight with primary antibodies at 4˚C. The antibodies used were as follows: Anti-zonula occludens-1 (ZO-1; 1:1,000; cat. no. bs-1329R; BIOSS), anti-claudin-5 (1:1,000; product code ab131259; Abcam), anti-occludin (1:1,000; product code ab216327; Abcam), anti-Beclin-1 (1:2,000), anti-LC3B (1:1,000), anti-p62 (1:1,000; product code ab109012; Abcam), anti-phosphorylated (p)-PI3K (1:1,000; cat. no. bs-6417R; BIOSS), anti-PI3K (1:1,000; product code ab191606; Abcam), anti-p-AKT (1:2,000; cat. no. 4060S; Cell Signaling Technology, Inc.), anti-AKT (1:2,000; cat. no. 4685S; Cell Signaling Technology, Inc.), anti-p-mTOR (1:1,000; cat. no. 5536S; Cell Signaling Technology, Inc.) and anti-mTOR (1:1,000; cat. no. 2983S; Cell Signaling Technology, Inc.). The membranes were washed with TBS-Tween-20 (1:1,000) and incubated with secondary antibodies (1:5,000; cat. no. 33101ES60; Shanghai Yeasen Biotechnology Co., Ltd.) for 1 h at room temperature. The bands were visualized by ECL (EMD Millipore). The ImageJ software (version 1.47; National Institutes of Health) was used for densitometric analysis.

RNA isolation and reverse transcription-quantitative (RT-q) PCR. Total RNA was extracted from brain ischemic penumbra tissues and co-culture cells with TRIzol® reagent (Invitrogen; Thermo Fisher Scientific, Inc.) and first strand cDNA was synthesized using a reverse transcription kit (PrimeScript™ RT Reagent kit-Perfect Real-Time; Takara Bio, Inc.). The kit was used according to the manufacturer's protocol. GAPDH was used as the control. The SYBR Green PCR Master Mix kit (Takara Biotechnology co., Ltd.) was used for RT-qPCR analysis. The thermocycling conditions were as follows: Initial denaturation at 95˚C for 8 min, 40 cycles of denaturation at 95˚C for 15 sec, annealing at 55˚C for 30 sec and extension at 70˚C for 25 sec. The relative expression of mRNA was analyzed using the $2^{-\Delta\Delta Cq}$ method (49). The primers used were as follows: Beclin-1 forward, 5'-CTGCATTGGCTACCAGCC CAG-3' and reverse, 5'-TCCTCACCACTCGGGCTCA-3'; LC3B forward, 5'-AGTCTCGATAAAGTGCCACG-3' and reverse, 5'-GGGCACCATATCGGCCATCA-3'; p62 forward, 5'-TGCAGGGCTACCTCACACTC-3' and reverse, 5'-AAC CTCACTCAGCGTGTCCA-3'; and GAPDH forward, 5'-AGT GCCTCGGTCGTCTCATA-3' and reverse, 5'-ATGAAGGGG TGCAGGATGGC-3'.

Statistical analysis. The data are expressed as the mean ± SD. Statistical analysis was performed using SPSS 20.0 (IBM Corp.). To analyze the difference between means, one-way ANOVA and Kruskal Wallis test with a least significant difference post hoc test was performed, such as Dunnett's and Tukey's post hoc tests. $P<0.05$ was considered to indicate a statistically significant difference. Each experiment was repeated at least three times.

Results

Selenium attenuates cerebral I/R injury in diabetic rats. The flow diagram of the *in vivo* experiment is illustrated in Fig. 1A. To investigate whether selenium exerted a protective effect on rats during I/R injury in hyperglycemic conditions, diabetic rats were subjected to MCAO, and the neurological deficit score, infarct volume, brain water content and pathological changes were analyzed 24 h later. The neurological deficit score of the HIR group was significantly higher than that of the Sham group after 24 h of I/R. Conversely, neurological deficit scores in the Se, 3-MA and Se + 3-MA groups were significantly lower than those of the HIR group (Fig. 1B). Furthermore, selenium significantly reduced the brain water content (Fig. 1C) and infarct volume (Fig. 1D and E) compared with the HIR group, indicating that selenium therapy can reduce cerebral I/R injury in hyperglycemic conditions.

Selenium protects BBB integrity. To further investigate the protective effects of selenium, BBB permeability was assessed by measuring EB leakage. As anticipated, hyperglycemic animals subjected to MCAO revealed increased EB leakage after 24 h of reperfusion. Conversely, the Se and 3-MA groups revealed reduced EB leakage when compared with the HIR group (Fig. 2A).

The TJ proteins ZO-1, claudin-5 and occludin are important determinants of the integrity and paracellular permeability of the BBB (50). Their expression was assessed by western blot analysis, and it was revealed that TJ protein expression in the HIR group was significantly reduced when compared with the Sham group. Conversely, a significant increase in TJ protein expression was observed in the Se, 3-MA and Se + 3-MA groups when compared with the HIR group (Fig. 2B-E).

I/R injury in hyperglycemic conditions increases autophagy but selenium reverses this effect. To investigate the role of autophagy in I/R injury in hyperglycemic conditions, the expression of the autophagy-associated proteins Beclin-1, LC3B and p62 was assessed by western blot analysis and

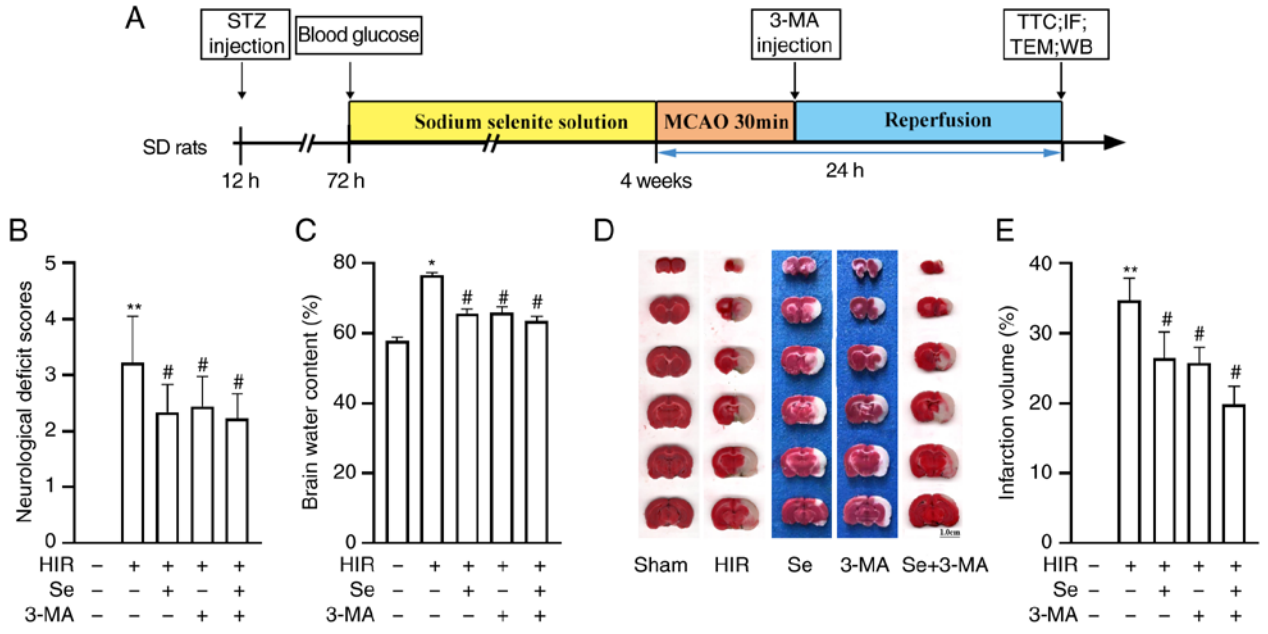

Figure 1. Selenium attenuates cerebral I/R injury in diabetic rats. (A) Flow diagram of the *in vivo* experiment. (B) Neurological deficit scores and (C) brain water content after 24 h of MCAO. (D) Representative triphenyltetrazolium chloride-stained slices. Pale areas correspond to infarcted tissues. (E) Bar-graph revealing infarct volumes (n=4 per group). Experiments were repeated 3 times for each condition. Scale bar, 1.0 cm. Results are expressed as the mean ± SD. *P<0.05 and **P<0.01 vs. the sham group; $^{\#}$P<0.05 vs. the HIR group. I/R, ischemia/reperfusion; MCAO, middle cerebral artery occlusion; HIR, hyperglycemia ischemia/reperfusion; TTC, triphenyltetrazolium chloride; STZ, streptozotocin; WB, western blotting; IF, immunofluorescence; TEM, transmission electron microscopy; 3-MA, 3-methyladenine; Se, sodium selenite.

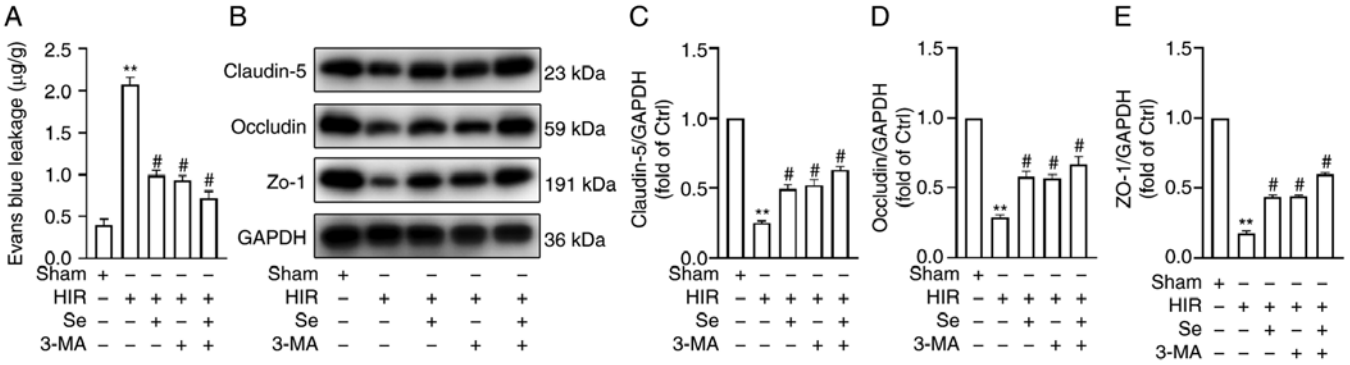

Figure 2. Effects of selenium on the permeability of the blood-brain barrier and tight junction protein expression. (A) Evans Blue leakage after 24 h of middle cerebral artery occlusion. (B) Representative western blots revealing levels of expression of ZO-1, claudin-5 and occludin in the ischemic penumbra. (C-E) Western blot analysis semi-quantification of claudin-5, occludin and ZO-1 levels. Results are expressed as the mean ± SD. **P<0.01 vs. the sham group; $^{\#}$P<0.05 vs. the HIR group. ZO-1, zonula occludens-1; HIR, hyperglycemia ischemia/reperfusion; 3-MA, 3-methyladenine; Se, sodium selenite.

immunofluorescence (n=4 per group). Immunofluorescence staining revealed an increased expression of Beclin-1 and LC3B, but a decreased expression of p62 (Fig. 3A-D) in the HIR group compared with the Sham group. Of note, selenium administration significantly decreased the expression of Beclin-1 and LC3B, but increased that of p62 (Fig. 3A-D). As revealed in Fig. 3E-I, the western blot analysis results confirmed the immunofluorescence data, since selenium significantly reduced the expression of Beclin-1 and LC3B, but increased that of p62.

BBB ultrastructural changes and autophagy were also evaluated by TEM. It was revealed that, in the Sham group, the BBB was intact, the mitochondrial morphology and plasma membrane were normal, and mitochondrial crests were arranged regularly. In the other four groups, the integrity of the BBB was compromised: The mitochondria exhibited different degrees of crest rupture, dissolution and vacuolation, and varying numbers of autophagosomes could be observed. The integrity of the BBB was damaged the most, and mitochondrial autophagosomes were most abundant in the HIR group. Conversely, the integrity of the BBB was only slightly compromised and the number of autophagosomes was decreased in the selenium-treated and 3-MA groups (Fig. 4A).

The expression of proteins associated with the PI3K pathway was also evaluated. A lower expression of p-PI3K/PI3K, p-AKT/AKT and p-mTOR/mTOR was observed in the HIR group compared with the Sham group. Of note, selenium reversed these changes (Fig. 4B-E). These results indicated that selenium has the same effects as 3-MA, suggesting that selenium reduces BBB damage following cerebral I/R injury in hyperglycemic conditions by inhibiting excessive autophagy.

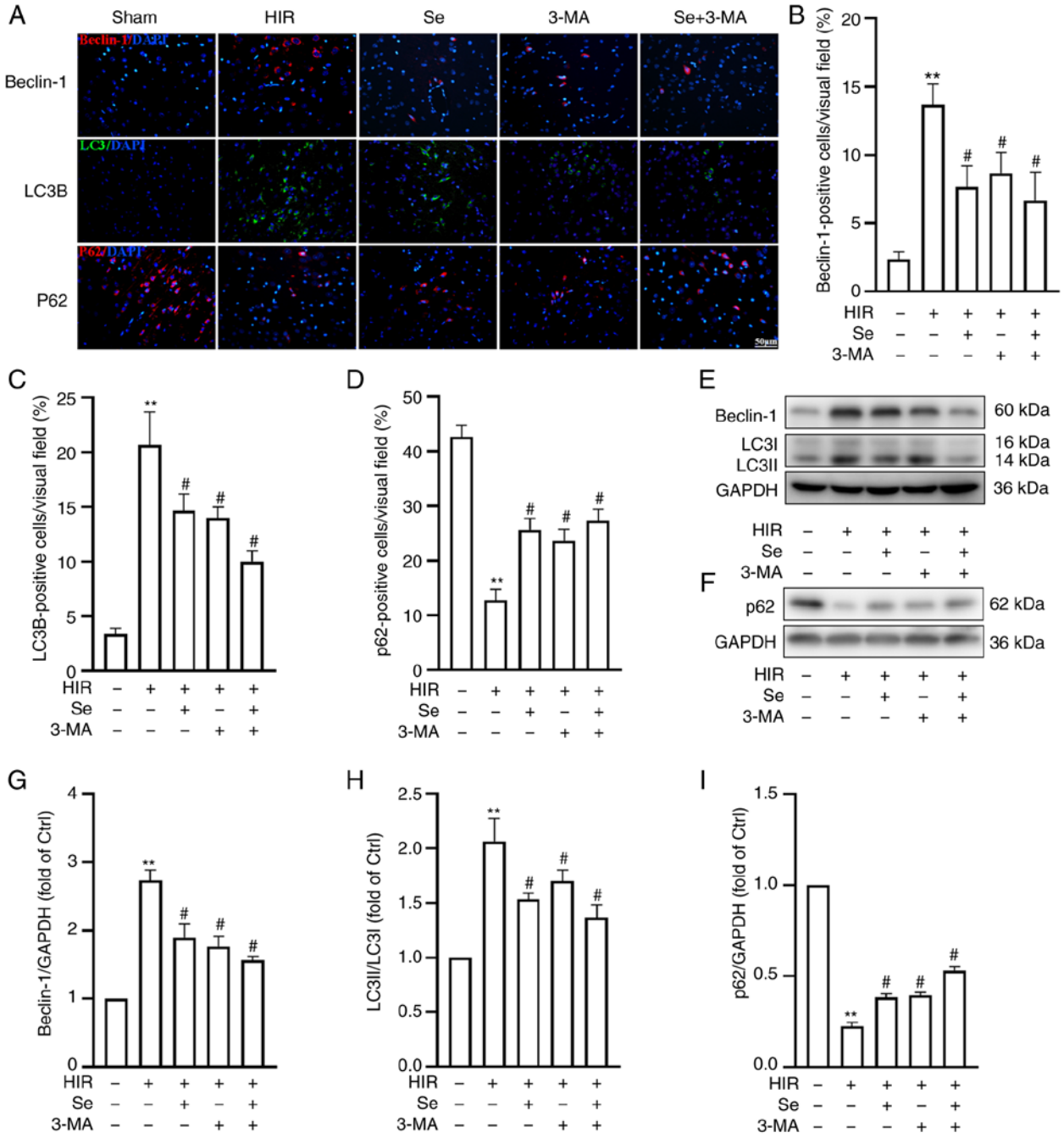

Figure 3. Effects of selenium on the expression of autophagy-associated proteins Beclin-1, LC3B and p62. (A) Immunofluorescence staining. Red color: Beclin-1, p62; Green color: LC3B; Blue color: DAPI nuclear staining. Scale bar, 50 μm. (B-D) The expression of Beclin-1, LC3B and p62 was assessed by immunofluorescence staining. (E and F) Representative western blots revealing the expression of Beclin-1, LC3B and p62 in the ischemic penumbra. (G-I) Western blot analysis semi-quantification of Beclin-1, LC3B and p62 expression. Results are expressed as the mean ± SD. **P<0.01 vs. the sham group; $^{\#}$P<0.05 vs. the HIR group. HIR, hyperglycemia ischemia/reperfusion; 3-MA, 3-methyladenine; Se, sodium selenite.

In vitro, selenium increases cell viability and protects the BBB, suppressing autophagy following OGD/R in hyperglycemic conditions. CD34 and GFAP are specific markers of brain microvascular endothelial cells and astrocytes, respectively (51,52). Immunofluorescence staining was used for bEnd.3 and MA-h cell identification (Fig. 5A and B). To determine the optimal concentrations of glucose and sodium selenite for the *in vitro* assays, cell viability was assessed using a CCK-8 assay. Co-cultured cells were treated with different concentrations of D-glucose for 24 h. The results revealed that the co-cultured cells were significantly damaged when the concentration of D-glucose reached 50 mM (Fig. 6A cell viability: 56.4±2.6%; P<0.05 vs. the control). Therefore, 50 mM D-glucose was used for the subsequent experiments. As revealed in Fig. 6B, selenium exerted a protective effect under hyperglycemic conditions and after OGD/R injury (cell viability in 100 nmol selenium: 89.2±2.7%, P<0.05 vs. the H + O group). There was no significant difference in cell viability between the 100 nmol selenium and control groups, indicating that selenium itself had no toxic effects on the co-cultured cells. The protective effects of selenium peaked at 100 nmol, and thus, this concentration was used for the subsequent experiments.

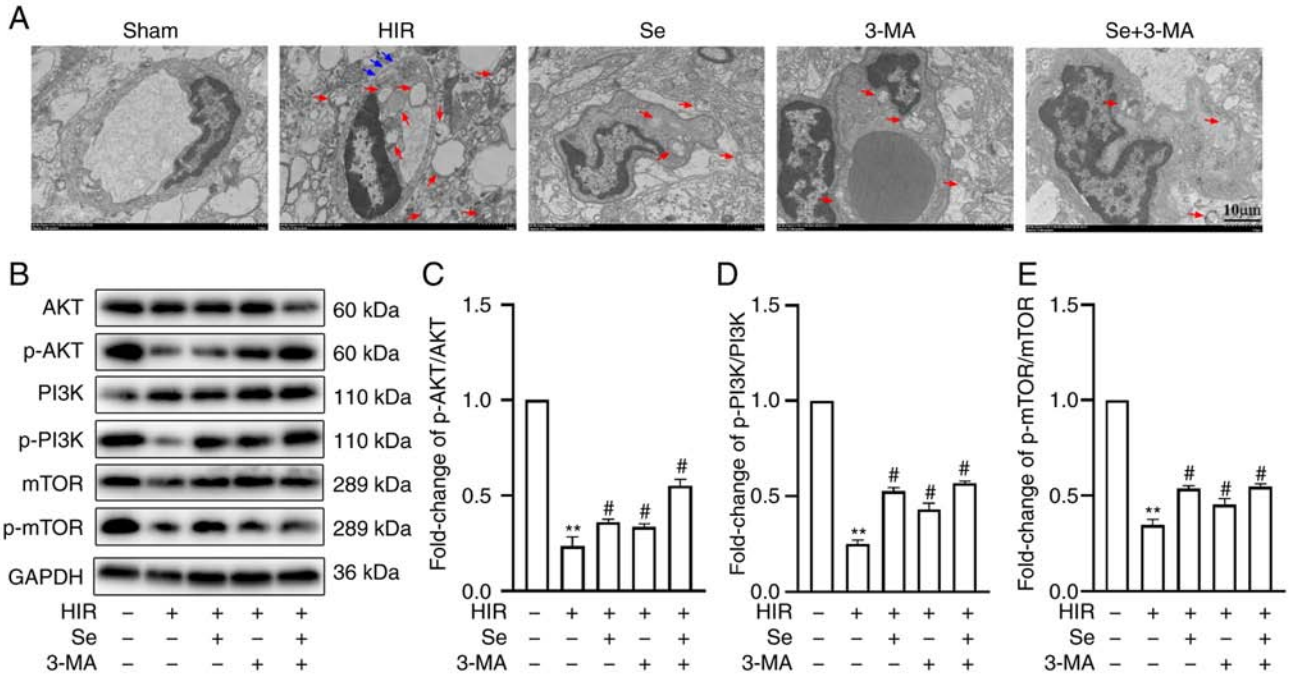

Figure 4. Pathological changes in brain tissue after 24 h of middle cerebral artery occlusion and effects of selenium on the expression of PI3K pathway proteins. (A) Pathological changes in ischemic penumbra (blue arrows indicate the continuity of endothelial cells; red arrows indicate mitochondria and autophagic vacuole). (B) Representative western blots showing the expression of p-PI3K/PI3K, p-AKT/AKT and p-mTOR/mTOR. (C-E) Western blot analysis semi-quantification of p-PI3K/PI3K, p-AKT/AKT and p-mTOR/mTOR. Results are expressed as the mean ± SD. **P<0.01 vs. the sham group; $^{\#}$P<0.05 vs. HIR group. p-, phosphorylated; HIR, hyperglycemia ischemia/reperfusion; 3-MA, 3-methyladenine; Se, sodium selenite.

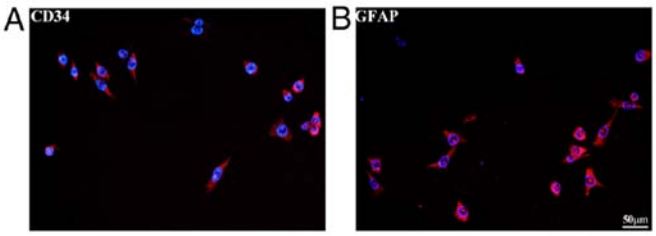

Figure 5. MA-h and bEnd.3 cell identification. (A) CD34 represents bEnd.3. (B) GFAP represents MA-h cells. Red color: CD34. GFAP: Blue color. DAPI nuclear staining. Scale bar, 50 μm. GFAP, glial fibrillary acid protein.

To further investigate the protective effects of selenium against BBB damage, cell viability and BBB permeability were assessed in the control, H + O, Se, 3-MA and Se + 3-MA groups. Hyperglycemia and OGD/R decreased cell viability (Fig. 6C) and increased permeability to sodium fluoride (Fig. 6D) when compared with the control group. Conversely, selenium increased cell viability (Fig. 6C) and decreased permeability to sodium fluoride following OGD/R under hyperglycemic conditions (Fig. 6D).

Furthermore, ZO-1, occludin and claudin-5 expression was significantly decreased following OGD/R under hyperglycemic conditions, as determined by western blot analysis. Conversely, selenium increased the levels of expression of these TJ proteins compared with the H + O group (Fig. 6E-H). These results indicated that selenium protects the BBB following OGD/R under hyperglycemic conditions *in vitro*.

Conversely, selenium reduced Beclin-1 and LC3B expression but increased that of p62 compared with the H + O group (Fig. 6I-M). These results were consistent with the *in vivo* results and indicated that selenium may protect the integrity of the BBB by inhibiting autophagy.

PI3K pathway inhibition reduces the protective effects of selenium. To explore the mechanisms underlying the protective effects of selenium on the BBB, cell viability, fluorescein leakage and TJ protein expression were assessed following the addition of Wort (a specific PI3K inhibitor) and insulin-like growth factor 1 (IGF-1; a PI3K activator). The cells were divided into the following groups: Vehicle (H + O + vehicle), Se, IGF-1, Wort and Se + Wort groups. Following treatment with selenium, cell viability increased (Fig. 7A) and permeability to sodium fluoride decreased (Fig. 7B) compared with the vehicle group, which was similar to the result following treatment with IGF-1. Conversely, Wort counteracted the beneficial effects of selenium.

In addition, TJ protein expression in the Wort group decreased significantly compared with the Se and IGF-1 groups (Fig. 7C-F). These results indicated that selenium improved BBB function through the PI3K signaling pathway.

Pharmacologic modulation of the PI3K signaling pathway enhances or inhibits autophagy following OGD/R under hyperglycemic conditions. To gain further insights into the mechanisms underlying the protective effects of selenium on the BBB, the PI3K signaling pathway was pharmacologically modulated and the expression of autophagy-related proteins was evaluated by western blot analysis. It was revealed that IGF-1 markedly increased the p-PI3K/PI3K, p-AKT/AKT and p-mTOR/mTOR ratios compared with the vehicle group. (Fig. 8A-D). Conversely, PI3K pathway protein expression was decreased following the addition of Wort (Fig. 8A-D).

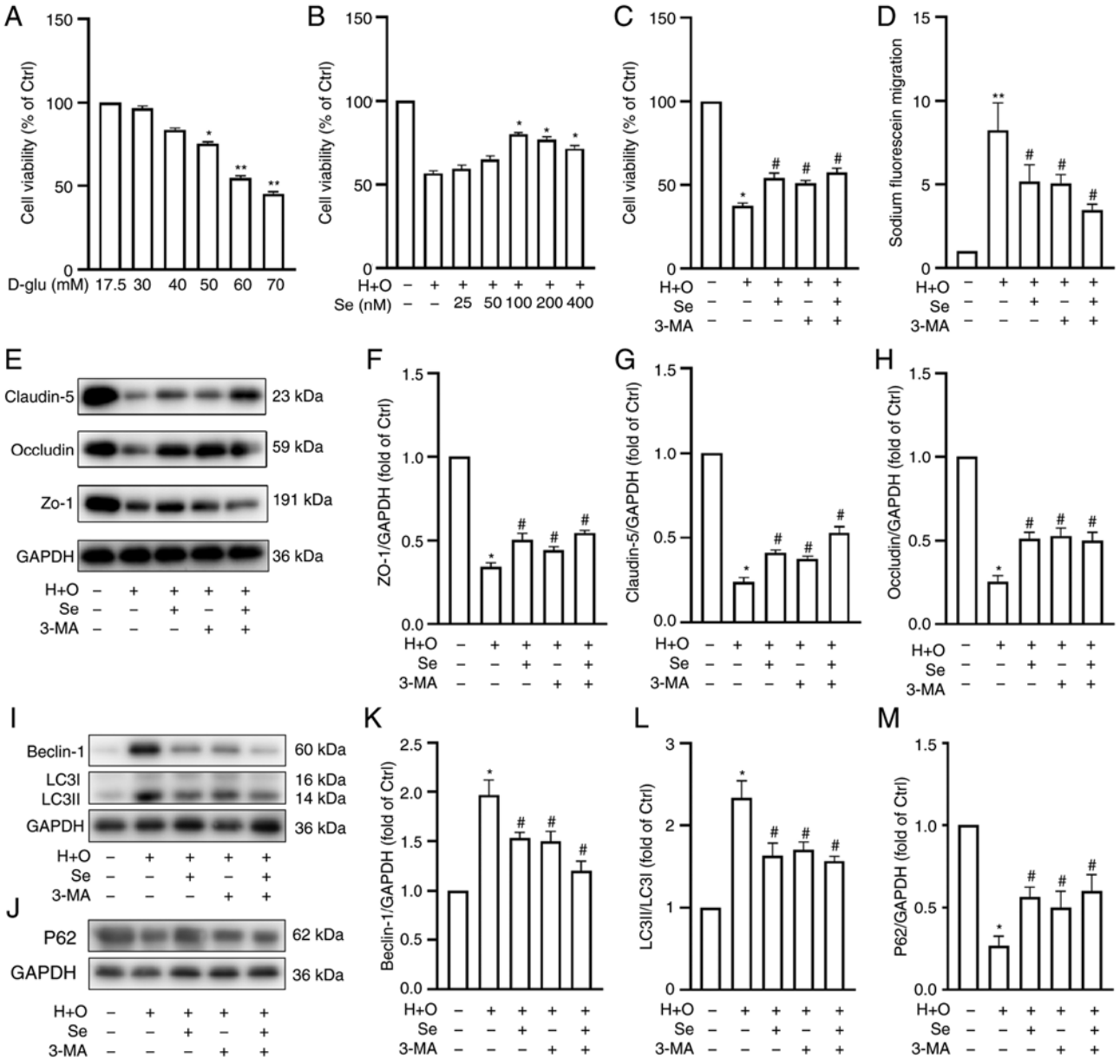

Figure 6. Effects of selenium on cell viability, fluorescein leakage and expression of TJ and autophagy-related proteins *in vitro*. Cell viability under different (A) D-glucose and (B) selenium concentrations, and (C) after 24 h of reoxygenation following 1 h of OGD plus 50 mM glucose (H + O). Sodium selenite, 100 nM; and 3-methyladenine, 50 nM. (D) Fluorescein leakage after OGD/R in hyperglycemic conditions. (E) Representative western blots revealing TJ protein expression. (F-H) Western blot analysis semi-quantification of TJ proteins. (I and J) Western blots revealing Beclin-1, LC3B and p62 expression. (K-M) Western blot analysis semi-quantification of Beclin-1, LC3B and p62. Experiments were repeated 3 times for each condition and each time-point. Results are expressed as the mean ± SD. *P<0.05 and **P<0.01 vs. the control group; $^{\#}$P<0.05 vs. the H + O group. TJ, tight junction; OGD/R, oxygen-glucose deprivation/reoxygenation; 3-MA, 3-methyladenine; Se, sodium selenite.

Furthermore, the expression levels of the autophagy proteins Beclin-1 and p62 were assessed by western blot analysis and RT-qPCR. The results revealed that IGF-1 decreased the expression of Beclin-1, but increased that of p62 (Fig. 8E-H), while Wort had the opposite effects. Similar results were observed in terms of Beclin-1 and p62 mRNA expression (Fig. 8I and J). In conclusion, the activation or inhibition of the PI3K pathway was revealed to downregulate or upregulate autophagy, respectively.

Selenium inhibits autophagy by activating the PI3K/AKT/mTOR signaling pathway. To verify whether selenium inhibits autophagy through the activation of the PI3K/AKT/mTOR signaling pathway, PI3K signaling pathway protein expression was assessed by western blot analysis following the addition of Wort. A clear reduction was identified in the Se + Wort group when compared with the Se group (Fig. 8A-D). Furthermore, the addition of Wort significantly increased the expression of Beclin-1 but decreased that of p62 (Fig. 8E-H). Consistent with the western blot analysis results, Beclin-1 mRNA levels were significantly upregulated and p62 levels were downregulated (Fig. 8I and J). In conclusion, the pharmacological inhibition of the PI3K pathway neutralized the selenium-induced effects on autophagy, suggesting that selenium acts through the PI3K signaling pathway.

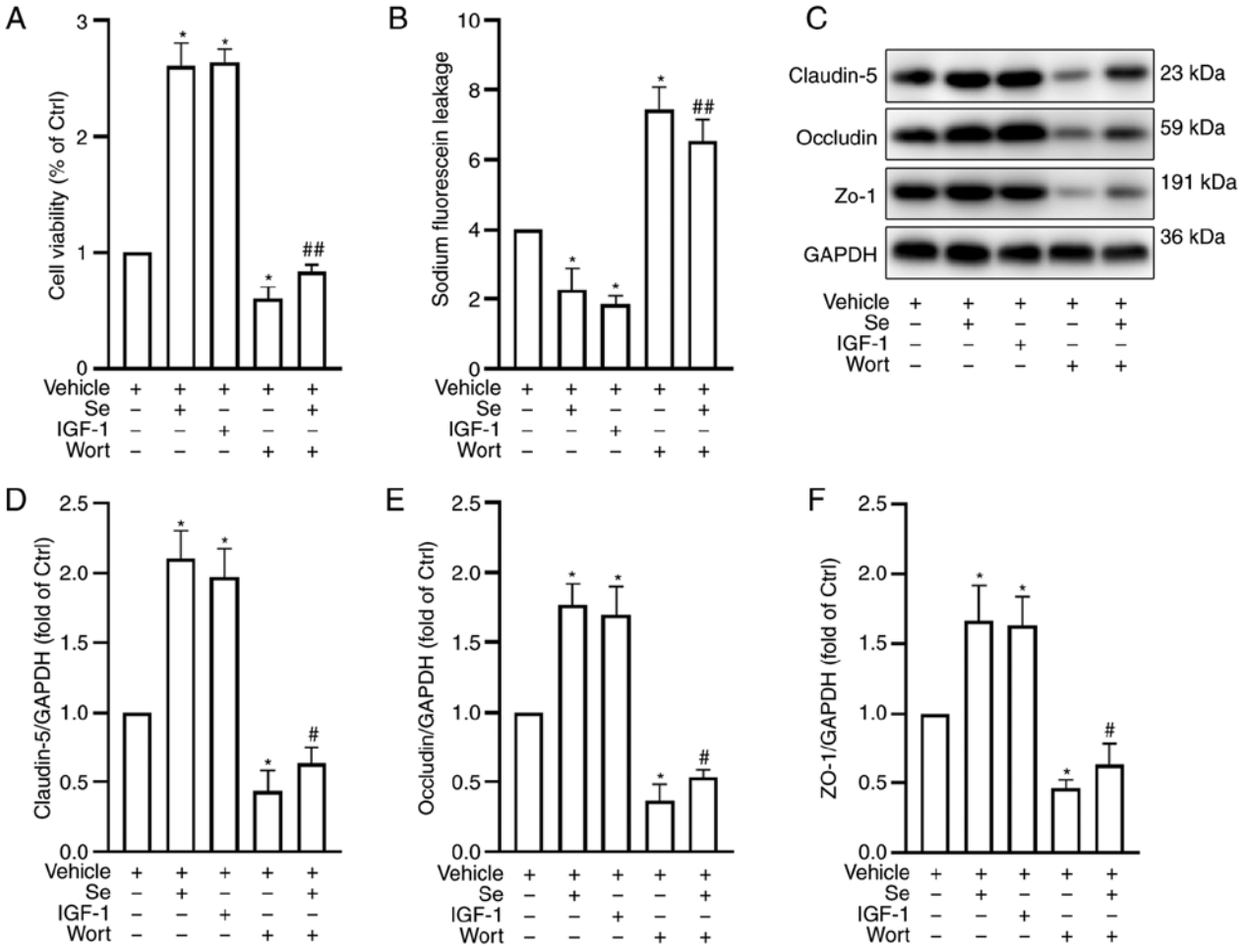

Figure 7. Inhibition of the PI3K pathway counteracts the protective effects of selenium. (A) Cell viability following treatment with sodium selenite (100 nM), wortmannin (10 nM) and insulin-like growth factor 1 (50 nM). (B) Fluorescein leakage across the blood-brain barrier following oxygen-glucose deprivation (1 h)/reoxygenation (24 h) in hyperglycemic conditions *in vitro*. (C) TJ protein expression was assessed by western blot analysis. (D-F) Western blot analysis semi-quantification of TJ proteins. Results are expressed as the mean ± SD. *P<0.05 vs. the vehicle group; $^{\#}$P<0.05 and $^{\#\#}$P<0.01 vs. the Se group. IGF-1, insulin-like growth factor 1; Se, sodium selenite; TJ, tight junction; Wort, wortmannin; ZO-1, zonula occludens-1.

Discussion

To the best of our knowledge, this is the first study demonstrating that selenium significantly reduces cerebral I/R injury-induced BBB damage in diabetic rats by inhibiting autophagy through the PI3K/AKT/mTOR signaling pathway.

Ischemic stroke is one of the main causes of disability worldwide. High glucose is an important risk factor for ischemic stroke. Acute hyperglycemia and chronic diabetes can aggravate this condition (53). High glucose levels can lead to microangiopathy, including thickening of the capillary basement membrane, changes in the intercellular charges and an increase in vascular permeability (54). Collectively, these factors can lead to a high incidence of ischemic stroke. Experimental studies have revealed that, compared with non-diabetic ischemic stroke, diabetic stroke can lead to more serious vascular dysfunction and inflammatory response and result in damage to the brain parenchyma (55,56). Currently, the treatment modalities for stroke in diabetic patients are relatively limited, whereas the disability and fatality rates in these patients are significantly increased (11).

As a physical diffusion barrier, the BBB prevents harmful substances from entering the brain tissue through the blood. The destruction of the BBB is a common clinical manifestation of CNS diseases, including stroke, and one of the causes of secondary damage to the brain parenchyma (57). During a stroke, the hypoxic microenvironment is formed by the whole penumbra after cerebral ischemia injury, resulting in BBB damage and increased permeability due to the interruption of the blood supply; BBB injury occurs in the acute phase after a stroke and is one of the first steps in the aggravation of stroke damage (4). However, there are few studies on the role of BBB in the pathology of stroke. Therefore, regulating the permeability of the BBB to protect the CNS from secondary injury may be a potential strategy for the treatment of CNS diseases, including stroke. Several experimental studies have revealed that damage to the BBB leads to increased permeability and hemorrhagic transformation in diabetic animals (55,58,59). The BBB is composed of endothelial cells, astrocytic terminal processes, pericytes and a basement membrane, which prevent microscopic and neurotoxic substances from entering the CNS (60). TJs between the endothelial cells form a diffusion barrier. These TJs are formed by proteins such as ZO-1, occludin and claudin-5 (61). TJs in mice with type 2 diabetes were revealed to be damaged following a stroke, increasing the infarcted area and aggravating the neurological function

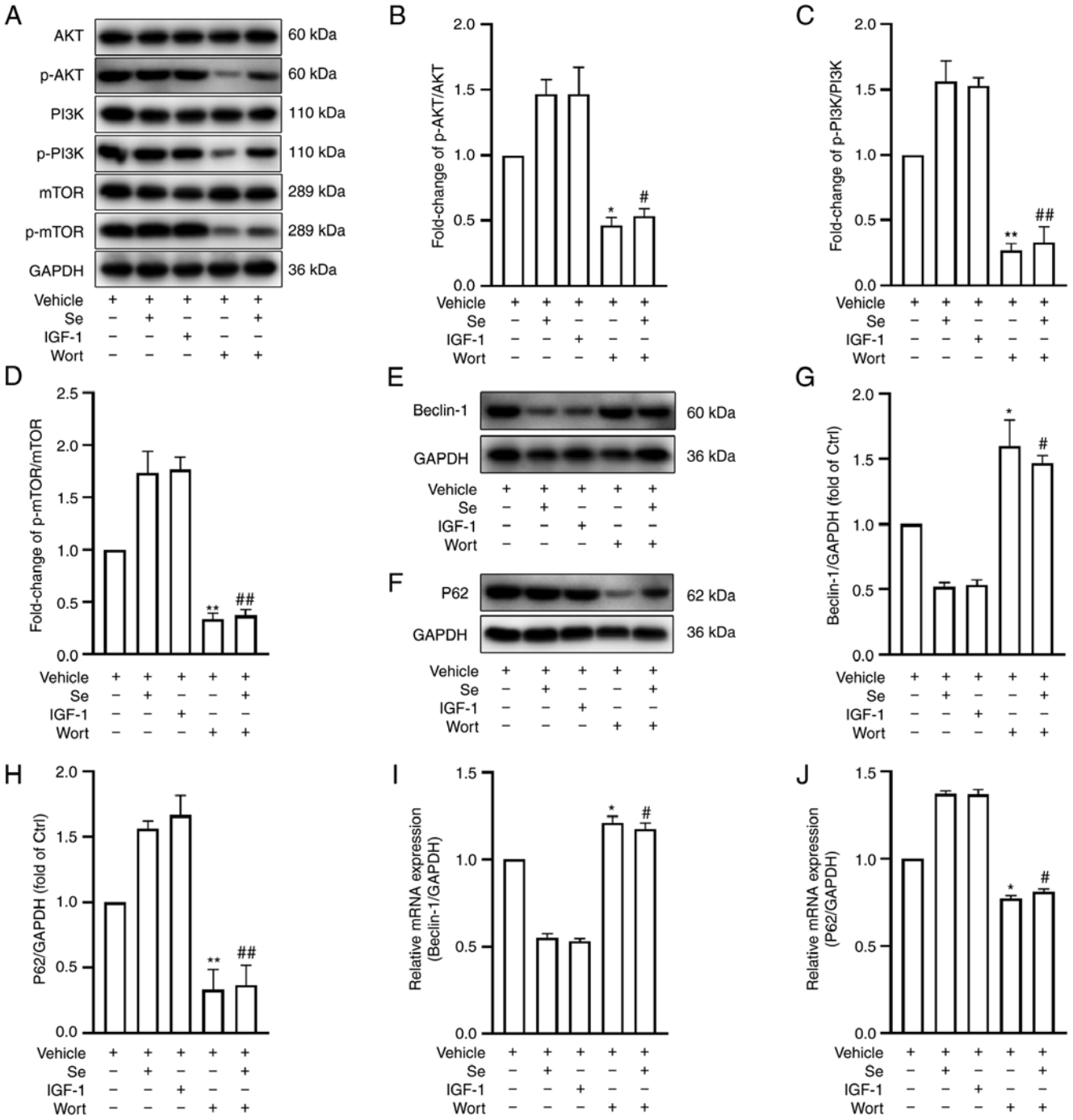

Figure 8. Inhibition of the PI3K signaling pathway neutralizes the selenium-mediated inhibition of autophagy. (A) The levels of p-PI3K/PI3K, p-AKT/AKT and p-mTOR/mTOR were assessed by western blot analysis. (B-D) Western blot analysis semi-quantification of p-PI3K/PI3K, p-AKT/AKT and p-mTOR/mTOR proteins. (E and F) The protein expression of Beclin-1 and p62 was examined by western blot analysis. (G and H) Western blot analysis semi-quantification of Beclin-1 and p62 protein expression. (I and J) Representative Beclin-1 and p62 mRNA levels. Results are expressed as the mean ± SD. *P<0.05 and **P<0.01 between the IGF-1 and Wort groups; $^{\#}$P<0.05 and $^{\#\#}$P<0.01 between the Se and Se + Wort groups. p-, phosphorylated; IGF-1, insulin-like growth factor 1; Wort, wortmannin; Se, sodium selenite.

defects (62). The results of the present study revealed that the integrity of the BBB was compromised following I/R injury in hyperglycemic conditions. Both *in vivo* and *in vitro* experiments revealed that the expression of TJ proteins decreased, while the permeability of the BBB increased. The expression of TJs was decreased in diabetic rats after cerebral I/R (P<0.01), whereas the expression of TJs was increased after selenium intervention (P<0.05) *in vitro*. Selenium treatment could increase the expression of TJ proteins, reduce EB leakage and improve the cell viability of brain microvascular endothelial cells, thereby reducing damage to the BBB. It is possible that *in vitro,* the co-cultured cells could not completely simulate BBB injury after HIR *in vivo*. The construction of BBB *in vitro* will be further improved in our future studies to render it more consistent with the ischemic microenvironment *in vivo*.

Autophagy is a physiological process that maintains the stability of the intracellular environment that degrades and recovers damaged proteins and organelles through the lysosomal

pathway. Autophagy plays a central role in several physiological and pathological processes (63,64). The autophagic process can be activated by nutritional deprivation or other stressful conditions. Previous studies have revealed that autophagy is upregulated following cerebral I/R in diabetes (2,65,66). Autophagy is characterized by the formation of autophagosomes that can engulf cytosolic organelles. Beclin-1, LC3B and p62 are the main autophagy-related proteins (67,68). Beclin-1 triggers autophagy and LC3B forms autophagosomes, whereas p62 is negatively correlated with autophagic activity (69). Growing evidence has indicated that overactivated autophagy under pathological conditions can trigger cell death and BBB damage; for example, following a stroke in diabetic mice, the expression of autophagy-related proteins was increased, while that of the TJ protein occludin was decreased, and 3-MA reversed these effects (70,71). Wu *et al* reported that Dl-3n-butylphthalide can exert neuroprotective effects by inhibiting autophagy and blocking TJ protein loss (72). Our previous study also revealed that hyperglycemia increased LC3 II/I expression following cerebral I/R injury (34). In the present study, it was revealed that the expression levels of Beclin-1 and LC3 were increased in diabetic rats after an ischemic stroke, whereas that of p62 was decreased, which was consistent with our previous results. However, selenium significantly attenuated these changes. In the *in vivo* experiment, the expression of the autophagy-related proteins Beclin-1 and LC3 II/I was significantly decreased, whereas that of p62 was significantly increased following selenium treatment. Similarly, following the use of the autophagy inhibitor 3-MA, selenium reduced autophagy and diabetic cerebral I/R injury. Selenium inhibited the expression of autophagy-related proteins *in vitro*. Furthermore, the expression of the PI3K/AKT/mTOR autophagy-related pathway proteins was also detected *in vivo*, and it was revealed that the expression of PI3K/AKT/mTOR-related pathway proteins was increased following treatment with sodium selenite. These findings indicated that selenium may inhibit autophagy through the PI3K signaling pathway.

The PI3K/AKT/mTOR signaling pathway regulates several biological processes, such as cell proliferation, differentiation and apoptosis, and is closely associated with autophagy (73). Nicotine can inhibit autophagy in brain microvascular endothelial cells by activating the PI3K/AKT/mTOR pathway (24). Homocysteine plays a neuroprotective role by inhibiting the excessive autophagy of neural stem cells following OGD/R through the PI3K/AKT/mTOR signaling pathway (74). In the *in vivo* results of the present study, it was revealed that the phosphorylation levels of the PI3K, AKT and mTOR proteins were significantly decreased following cerebral I/R injury under high glucose conditions, but selenium significantly inhibited these effects. However, it was unclear whether selenium affected autophagy through the PI3K/Akt/mTOR signaling pathway. Therefore, an *in vitro* study was designed and conducted, using the PI3K/Akt/mTOR signaling pathway specific activator, IGF-1, and the specific inhibitor Wort, to further determine whether there was a causal relationship between selenium and the PI3K/Akt/mTOR signaling pathway. The selenium-mediated effects were accompanied by corresponding changes in the expression of autophagy-related proteins. Of note, Wort, a PI3K inhibitor, counteracted the beneficial effects of selenium following BBB damage. These results indicated that selenium attenuated cerebral I/R injury-induced BBB damage under hyperglycemic conditions by inhibiting autophagy through the PI3K/AKT/mTOR signaling pathway.

The present study had certain limitations. Although it was demonstrated herein that selenium can reduce damage to the BBB during the acute phase of cerebral I/R injury under hyperglycemic conditions, whether selenium can also protect the BBB in the subacute and chronic phases after stroke needs to be evaluated in future studies.

In conclusion, the results of the present study revealed that selenium significantly ameliorated I/R injury-induced BBB damage under hyperglycemic conditions, both *in vivo* and *in vitro*, by activating the PI3K/AKT/mTOR pathway to inhibit overactive autophagy.

Acknowledgements

Not applicable.

Funding

The present study was supported by the National Natural Science Foundation of China (grant no. 3196070051).

Availability of data and materials

The datasets used and/or analyzed during the current study are available from the corresponding author on reasonable request.

Authors' contributions

BY, YL and YM contributed to the conception and design of this study. BY, XZ and LY performed the experiments. XS and LJ analysed the data and wrote the manuscript. JZ reviewed the manuscript for important intellectual content. BY and LJ confirmed the authenticity of all the raw data. All authors read and approved the final manuscript.

Ethics approval and consent to participate

All animal procedures were approved by the Institutional Animal Care and Use Committee (IACUC) of the Ningxia Medical University (Yinchuan, China).

Patient consent for publication

Not applicable.

Competing interests

The authors declare that they have no competing interests.

References

1. Liu MB, Wang W, Gao JM, Li F, Shi JS and Gong QH: Icariside II attenuates cerebral ischemia/reperfusion-induced blood-brain barrier dysfunction in rats via regulating the balance of MMP9/TIMP1. Acta Pharmacol Sin 41: 1547-1556, 2020.
2. Gao J, Long L, Xu F, Feng L, Liu Y, Shi J and Gong Q: Icariside II, a phosphodiesterase 5 inhibitor, attenuates cerebral ischaemia/reperfusion injury by inhibiting glycogen synthase kinase-3β-mediated activation of autophagy. Br J Pharmacol 177: 1434-1452, 2020.

3. Wu C, Chen J, Yang R, Duan F, Li S and Chen X: Mitochondrial protective effect of neferine through the modulation of nuclear factor erythroid 2-related factor 2 signalling in ischaemic stroke. Br J Pharmacol 176: 400-415, 2019.
4. Venkat P, Chopp M and Chen J: Blood-brain barrier disruption, vascular impairment, and ischemia/reperfusion damage in diabetic stroke. J Am Heart Assoc 6: e005819, 2017.
5. Shou J, Zhou L, Zhu S and Zhang X: Diabetes is an independent risk factor for stroke recurrence in stroke patients: A meta-analysis. J Stroke Cerebrovasc Dis 24: 1961-1968, 2015.
6. Chen J, Cui X, Zacharek A, Cui Y, Roberts C and Chopp M: White matter damage and the effect of matrix metalloproteinases in type 2 diabetic mice after stroke. Stroke 42: 445-452, 2011.
7. Zhang X, Wei M, Fan J, Yan W, Zha X, Song H, Wan R, Yin Y and Wang W: Ischemia-induced upregulation of autophagy preludes dysfunctional lysosomal storage and associated synaptic impairments in neurons. Autophagy 17: 1519-1542, 2021.
8. Chen J, Ye X, Yan T, Zhang C, Yang XP, Cui X, Cui Y, Zacharek A, Roberts C, Liu X, *et al*: Adverse effects of bone marrow stromal cell treatment of stroke in diabetic rats. Stroke 42: 3551-3558, 2011.
9. Wang W, Li M, Chen Q and Wang J: Hemorrhagic transformation after tissue plasminogen activator reperfusion therapy for ischemic stroke: Mechanisms, models, and biomarkers. Mol Neurobiol 52: 1572-1579, 2015.
10. Karatas H, Eun Jung J, Lo EH and van Leyen K: Inhibiting 12/15-lipoxygenase to treat acute stroke in permanent and tPA induced thrombolysis models. Brain Res 1678: 123-128, 2018.
11. Muir KW: Stroke in 2015: The year of endovascular treatment. Lancet Neurol 15: 2-3, 2016.
12. Zhang Y, Cao Y and Liu C: Autophagy and ischemic stroke. Adv Exp Med Biol 1207: 111-134, 2020.
13. Puyal J, Vaslin A, Mottier V and Clarke PG: Postischemic treatment of neonatal cerebral ischemia should target autophagy. Ann Neurol 66: 378-389, 2009.
14. Wei K, Wang P and Miao CY: A double-edged sword with therapeutic potential: An updated role of autophagy in ischemic cerebral injury. CNS Neurosci Ther 18: 879-886, 2012.
15. Feng D, Wang B, Wang L, Abraham N, Tao K, Huang L, Shi W, Dong Y and Qu Y: Pre-ischemia melatonin treatment alleviated acute neuronal injury after ischemic stroke by inhibiting endoplasmic reticulum stress-dependent autophagy via PERK and IRE1 signalings. J Pineal Res 62, 2017.
16. Yang Z, Lin P, Chen B, Zhang X, Xiao W, Wu S, Huang C, Feng D, Zhang W and Zhang J: Autophagy alleviates hypoxia-induced blood-brain barrier injury via regulation of CLDN5 (claudin 5). Autophagy: 1-20, 2020 (Online ahead of print).
17. Li H, He Y, Zhang C, Ba T, Guo Z, Zhuo Y, He L and Dai H: NOX1 down-regulation attenuated the autophagy and oxidative damage in pig intestinal epithelial cell following transcriptome analysis of transport stress. Gene 763: 145071, 2020.
18. Kim KA, Kim D, Kim JH, Shin YJ, Kim ES, Akram M, Kim EH, Majid A, Baek SH and Bae ON: Autophagy-mediated occludin degradation contributes to blood-brain barrier disruption during ischemia in bEnd.3 brain endothelial cells and rat ischemic stroke models. Fluids Barriers CNS 17: 21, 2020.
19. Zhang Y, Zhang X, Wei Q, Leng S, Li C, Han B, Bai Y, Zhang H and Yao H: Activation of sigma-1 receptor enhanced pericyte survival via the interplay between apoptosis and autophagy: Implications for blood-brain barrier integrity in stroke. Transl Stroke Res 11: 267-287, 2020.
20. Wei N, Yu SP, Gu XH, Chen DD, Whalin MK, Xu GL, Liu XF and Wei L: The involvement of autophagy pathway in exaggerated ischemic brain damage in diabetic mice. CNS Neurosci Ther 19: 753-763, 2013.
21. Che H, Li H, Li Y, Wang YQ, Yang ZY, Wang RL and Wang LH: Melatonin exerts neuroprotective effects by inhibiting neuronal pyroptosis and autophagy in STZ-induced diabetic mice. FASEB J 34: 14042-14054, 2020.
22. Fu B, Zeng Q, Zhang Z, Qian M, Chen J, Dong W and Li M: Epicatechin gallate protects HBMVECs from ischemia/reperfusion injury through ameliorating apoptosis and autophagy and promoting neovascularization. Oxid Med Cell Longev 2019: 7824684, 2019.
23. Wei R, Liu H, Chen R, Sheng Y and Liu T: Astragaloside IV combating liver cirrhosis through the PI3K/Akt/mTOR signaling pathway. Exp Ther Med 17: 393-397, 2019.
24. Wu C, Yang M, Liu R, Hu H, Ji L, Zhang X, Huang S and Wang L: Nicotine reduces human brain microvascular endothelial cell response to *Escherichia coli* K1 infection by inhibiting autophagy. Front Cell Infect Microbiol 10: 484, 2020.
25. Wang M, Li YJ, Ding Y, Zhang HN, Sun T, Zhang K, Yang L, Guo YY, Liu SB, Zhao MG and Wu YM: Silibinin prevents autophagic cell death upon oxidative stress in cortical neurons and cerebral ischemia-reperfusion injury. Mol Neurobiol 53: 932-943, 2016.
26. Liu YP, Shao SJ and Guo HD: Schwann cells apoptosis is induced by high glucose in diabetic peripheral neuropathy. Life Sci 248: 117459, 2020.
27. Liu Y, Chen X, Yao J and Kang J: Circular RNA ACR relieves high glucose-aroused RSC96 cell apoptosis and autophagy via declining microRNA-145-3p. J Cell Biochem, Dec 30, 2019 (Online ahead of print).
28. Arias-Borrego A, Callejón-Leblic B, Calatayud M, Gómez-Ariza JL, Collado MC and Garcia-Barrera T: Insights into cancer and neurodegenerative diseases through selenoproteins and the connection with gut microbiota-current analytical methodologies. Expert Rev Proteomics 16: 805-814, 2019.
29. Yang J, Hamid S, Cai J, Liu Q, Xu S and Zhang Z: Selenium deficiency-induced thioredoxin suppression and thioredoxin knock down disbalanced insulin responsiveness in chicken cardiomyocytes through PI3K/Akt pathway inhibition. Cell Signal 38: 192-200, 2017.
30. Zhang Z, Liu M, Guan Z, Yang J, Liu Z and Xu S: Disbalance of calcium regulation-related genes in broiler hearts induced by selenium deficiency. Avian Pathol 46: 265-271, 2017.
31. Zhang Q, Zhang C, Ge J, Lv MW, Talukder M, Guo K, Li YH and Li JL: Ameliorative effects of resveratrol against cadmium-induced nephrotoxicity via modulating nuclear xenobiotic receptor response and PINK1/Parkin-mediated mitophagy. Food Funct 11: 1856-1868, 2020.
32. Feng C, Li D, Chen M, Jiang L, Liu X, Li Q, Geng C, Sun X, Yang G, Zhang L and Yao X: Citreoviridin induces myocardial apoptosis through PPAR-γ-mTORC2-mediated autophagic pathway and the protective effect of thiamine and selenium. Chem Biol Interact 311: 108795, 2019.
33. Zhang C, Wang LL, Cao CY, Li N, Talukder M and Li JL: Selenium mitigates cadmium-induced crosstalk between autophagy and endoplasmic reticulum stress via regulating calcium homeostasis in avian leghorn male hepatoma (LMH) cells. Environ Pollut 265: 114613, 2020.
34. Lu C, Guo Y, Zhang Y, Yang L, Chang Y, Zhang JW, Jing L and Zhang JZ: Coenzyme Q10 ameliorates cerebral ischemia reperfusion injury in hyperglycemic rats. Pathol Res Pract 213: 1191-1199, 2017.
35. MacArthur Clark JA and Sun D: Guidelines for the ethical review of laboratory animal welfare People's Republic of China national standard GB/T 35892-2018 (issued 6 February 2018 effective from 1 September 2018). Animal Model Exp Med 3: 103-113, 2020.
36. Sun X, Wang D, Zhang T, Lu X, Duan F, Ju L, Zhuang X and Jiang X: Eugenol Attenuates cerebral ischemia-reperfusion injury by enhancing autophagy via AMPK-mTOR-P70S6K pathway. Front Pharmacol 11: 84, 2020.
37. Fan X, Qiu J, Yu Z, Dai H, Singhal AB, Lo EH and Wang X: A rat model of studying tissue-type plasminogen activator thrombolysis in ischemic stroke with diabetes. Stroke 43: 567-570, 2012.
38. Yang L, Ma YM, Shen XL, Fan YC, Zhang JZ, Li PA and Jing L: The involvement of mitochondrial biogenesis in selenium reduced hyperglycemia-aggravated cerebral ischemia injury. Neurochem Res 45: 1888-1901, 2020.
39. Liu L, Cen J, Man Y, Li J, Zhang D, Wang F, Li J, Ma J, Wang X and Ji B: Transplantation of human umbilical cord blood mononuclear cells attenuated ischemic injury in MCAO Rats via inhibition of NF-κB and NLRP3 inflammasome. Neuroscience 369: 314-324, 2018.
40. Yu Q, Li Q, Yang X, Liu Q, Deng J, Zhao Y, Hu R and Dai M: Dexmedetomidine suppresses the development of abdominal aortic aneurysm by downregulating the mircoRNA-21/PDCD 4 axis. Int J Mol Med 47: 90, 2021.
41. Xiong D, Deng Y, Huang B, Yin C, Liu B, Shi J and Gong Q: Icariin attenuates cerebral ischemia-reperfusion injury through inhibition of inflammatory response mediated by NF-κB, PPARα and PPARγ in rats. Int Immunopharmacol 30: 157-162, 2016.
42. Tureyen K, Bowen K, Liang J, Dempsey RJ and Vemuganti R: Exacerbated brain damage, edema and inflammation in type-2 diabetic mice subjected to focal ischemia. J Neurochem 116: 499-507, 2011.
43. Zhang G, Zhang T, Li N, Wu L, Gu J, Li C, Zhao C, Liu W, Shan L, Yu P, *et al*: Tetramethylpyrazine nitrone activates the BDNF/Akt/CREB pathway to promote post-ischaemic neuroregeneration and recovery of neurological functions in rats. Br J Pharmacol 175: 517-531, 2018.

44. Fang L, Li X, Zhong Y, Yu J, Yu L, Dai H and Yan M: Autophagy protects human brain microvascular endothelial cells against methylglyoxal-induced injuries, reproducible in a cerebral ischemic model in diabetic rats. J Neurochem 135: 431-440, 2015.
45. Tian X, Peng J, Zhong J, Yang M, Pang J, Lou J, Li M, An R, Zhang Q, Xu L and Dong Z: β-Caryophyllene protects in vitro neurovascular unit against oxygen-glucose deprivation and re-oxygenation-induced injury. J Neurochem 139: 757-768, 2016.
46. Mysiorek C, Culot M, Dehouck L, Derudas B, Staels B, Bordet R, Cecchelli R, Fenart L and Berezowski V: Peroxisome-proliferator-activated receptor-alpha activation protects brain capillary endothelial cells from oxygen-glucose deprivation-induced hyperpermeability in the blood-brain barrier. Curr Neurovasc Res 6: 181-193, 2009.
47. Liu M, Pi H, Xi Y, Wang L, Tian L, Chen M, Xie J, Deng P, Zhang T, Zhou C, *et al*: KIF5A-dependent axonal transport deficiency disrupts autophagic flux in trimethyltin chloride-induced neurotoxicity. Autophagy 17: 903-924, 2021.
48. Rastogi M and Singh SK: Zika virus NS1 affects the junctional integrity of human brain microvascular endothelial cells. Biochimie 176: 52-61, 2020.
49. Livak K and Schmittgen T: Analysis of relative gene expression data using real-time quantitative PCR and the 2(-Delta Delta C(T)) method. Methods 25: 402-408, 2001.
50. Manthari RK, Tikka C, Ommati MM, Niu R, Sun Z, Wang J, Zhang J and Wang J: Arsenic-induced autophagy in the developing mouse cerebellum: Involvement of the blood-brain Barrier's tight-junction proteins and the PI3K-Akt-mTOR signaling pathway. J Agric Food Chem 66: 8602-8614, 2018.
51. Franke H, Galla H and Beuckmann C: Primary cultures of brain microvessel endothelial cells: A valid and flexible model to study drug transport through the blood-brain barrier in vitro. Brain Res Brain Res Protoc 5: 248-256, 2000.
52. Hamprecht B and Löffler F: Primary glial cultures as a model for studying hormone action. Comparative Study 109: 341-345, 1985.
53. Lee KJ, Lee JS and Jung KH: Interactive effect of acute and chronic glycemic indexes for severity in acute ischemic stroke patients. BMC Neurol 18: 105, 2018.
54. Ji Q, Han J, Wang L, Liu J, Dong Y, Zhu K and Shi L: MicroRNA-34a promotes apoptosis of retinal vascular endothelial cells by targeting SIRT1 in rats with diabetic retinopathy. Cell Cycle 19: 2886-2896, 2020.
55. Tu Y, Guo C, Song F, Huo Y, Geng Y, Guo M, Bao H, Wu X and Fan W: Mild hypothermia alleviates diabetes aggravated cerebral ischemic injury via activating autophagy and inhibiting pyroptosis. Brain Res Bull 150: 1-12, 2019.
56. Kumari R, Bettermann K, Willing L, Sinha K and Simpson IA: The role of neutrophils in mediating stroke injury in the diabetic db/db mouse brain following hypoxia-ischemia. Neurochem Int 139: 104790, 2020.
57. Okada T, Suzuki H, Travis ZD and Zhang JH: The stroke-induced blood-brain barrier disruption: Current progress of inspection technique, mechanism, and therapeutic target. Curr Neuropharmacol 18: 1187-1212, 2020.
58. Li W, Qu Z, Prakash R, Chung C, Ma H, Hoda MN, Fagan SC and Ergul A: Comparative analysis of the neurovascular injury and functional outcomes in experimental stroke models in diabetic Goto-Kakizaki rats. Brain Res 1541: 106-114, 2013.
59. Venkat P, Zacharek A, Landschoot-Ward J, Wang F, Culmone L, Chen Z, Chopp M and Chen J: Exosomes derived from bone marrow mesenchymal stem cells harvested from type two diabetes rats promotes neurorestorative effects after stroke in type two diabetes rats. Exp Neurol 334: 113456, 2020.
60. Nian K, Harding IC, Herman IM and Ebong EE: Blood-brain barrier damage in ischemic stroke and its regulation by endothelial mechanotransduction. Front Physiol 11: 605398, 2020.
61. Tietz S and Engelhardt B: Brain barriers: Crosstalk between complex tight junctions and adherens junctions. J Cell Biol 209: 493-506, 2015.
62. Cui X, Chopp M, Zacharek A, Ye X, Roberts C and Chen J: Angiopoietin/Tie2 pathway mediates type 2 diabetes induced vascular damage after cerebral stroke. Neurobiol Dis 43: 285-292, 2011.
63. Shao Z, Dou S, Zhu J, Wang H, Xu D, Wang C, Cheng B and Bai B: The role of mitophagy in ischemic stroke. Front Neurol 11: 608610, 2020.
64. Xu W, Ocak U, Gao L, Tu S, Lenahan CJ, Zhang J and Shao A: Selective autophagy as a therapeutic target for neurological diseases. Cell Mol Life Sci 78: 1369-1392, 2021.
65. Chen L, Zhang B and Toborek M: Autophagy is involved in nanoalumina-induced cerebrovascular toxicity. Nanomedicine 9: 212-221, 2013.
66. Xiao Y, Fan M, Jin W, Li WA, Jia Y, Dong Y, Jiang X, Xu J, Meng N and Lv P: Lithium chloride ameliorated spatial cognitive impairment through activating mTOR phosphorylation and inhibiting excessive autophagy in the repeated cerebral ischemia-reperfusion mouse model. Exp Ther Med 20: 109, 2020.
67. Menzie-Suderam JM, Modi J, Xu H, Bent A, Trujillo P, Medley K, Jimenez E, Shen J, Marshall M, Tao R, *et al*: Granulocyte-colony stimulating factor gene therapy as a novel therapeutics for stroke in a mouse model. J Biomed Sci 27: 99, 2020.
68. Fu C, Zhang X, Lu Y, Wang F, Xu Z, Liu S, Zheng H and Liu X: Geniposide inhibits NLRP3 inflammasome activation via autophagy in BV-2 microglial cells exposed to oxygen-glucose deprivation/reoxygenation. Int Immunopharmacol 84: 106547, 2020.
69. Zhao B, Yuan Q, Hou JB, Xia ZY, Zhan LY, Li M, Jiang M, Gao WW and Liu L: Inhibition of HDAC3 ameliorates cerebral ischemia reperfusion injury in diabetic mice in vivo and in vitro. J Diabetes Res: 2019: 8520856, 2019.
70. Pan Q, Liu Y, Wang G, Wen Z and Wang Y: MTMR14 protects against cerebral stroke through suppressing PTEN-regulated autophagy. Biochem Biophys Res Commun 529: 1045-1052, 2020.
71. Nazarinia D, Aboutaleb N, Gholamzadeh R, Nasseri Maleki S, Mokhtari B and Nikougoftar M: Conditioned medium obtained from human amniotic mesenchymal stem cells attenuates focal cerebral ischemia/reperfusion injury in rats by targeting mTOR pathway. J Chem Neuroanat 102: 101707, 2019.
72. Wu F, Xu K, Xu K, Teng C, Zhang M, Xia L, Zhang K, Liu L, Chen Z, Xiao J, *et al*: Dl-3n-butylphthalide improves traumatic brain injury recovery via inhibiting autophagy-induced blood-brain barrier disruption and cell apoptosis. J Cell Mol Med 24: 1220-1232, 2020.
73. Heras-Sandoval D, Pérez-Rojas JM, Hernández-Damián J and Pedraza-Chaverri J: The role of PI3K/AKT/mTOR pathway in the modulation of autophagy and the clearance of protein aggregates in neurodegeneration. Cell Signal 26: 2694-2701, 2014.
74. Wang M, Liang X, Cheng M, Yang L, Liu H, Wang X, Sai N and Zhang X: Homocysteine enhances neural stem cell autophagy in in vivo and in vitro model of ischemic stroke. Cell Death Dis 10: 561, 2019.